

Learning Decentralized Routing Policies via Graph Attention-based Multi-Agent Reinforcement Learning in Lunar Delay-Tolerant Networks

Federico Lozano-Cuadra*, Beatriz Soret*, Marc Sanchez Net†, Abhishek Cauligi‡, and Federico Rossi†

Abstract—We present a fully decentralized routing framework for multi-robot exploration missions operating under the constraints of a Lunar Delay-Tolerant Network (LDTN). In this setting, autonomous rovers must relay collected data to a lander under intermittent connectivity and unknown mobility patterns. We formulate the problem as a Partially Observable Markov Decision Problem (POMDP) and propose a Graph Attention-based Multi-Agent Reinforcement Learning (GAT-MARL) policy that performs Centralized Training, Decentralized Execution (CTDE). Our method relies only on local observations and does not require global topology updates or packet replication, unlike classical approaches such as shortest path and controlled flooding-based algorithms. Through Monte Carlo simulations in randomized exploration environments, GAT-MARL provides higher delivery rates, no duplications, and fewer packet losses, and is able to leverage short-term mobility forecasts; offering a scalable solution for future space robotic systems for planetary exploration, as demonstrated by successful generalization to larger rover teams.

I. INTRODUCTION

The renewed interest in planetary and lunar surface exploration has accelerated the development of autonomous multi-robot systems. Missions such as Cooperative Autonomous Distributed Robotic Exploration (CADRE) [1], led by NASA’s Jet Propulsion Laboratory (JPL), aim to demonstrate high Technology Readiness Level (TRL) for cooperative autonomy in space robotics. In particular, CADRE plans to deploy a team of three rovers to explore the Reiner Gamma region of the Moon around a lander, which will serve as a base station and gateway to Earth.

However, these initial demonstrations assume that the exploring agents remain within the communication range of the lander, thereby simplifying network design because nodes (rovers and lander) can simply broadcast the information and assume all-to-all communication. In future science-driven missions, exploring agents will need to leave the lander’s coverage area to reach farther, uncharted regions. This shift introduces new challenges: nodes must operate autonomously as a Delay-Tolerant Network (DTN) [2], making

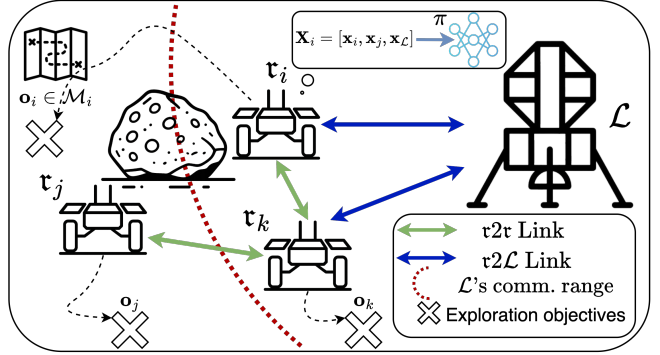


Fig. 1: Snapshot of a Lunar Delay Tolerant Network (LDTN) with three rovers $\tau \in \mathfrak{R}$ and a lander \mathcal{L} , which serves as the base station. Rovers τ_i and τ_k have direct connection with \mathcal{L} and with one another, whereas τ_j can only communicate with τ_k . Every rover explores a different sub-area of the map \mathcal{M} by defining objectives \mathbf{o} . Each τ collects a local observation $\mathbf{X}_\tau = [\mathbf{x}_n]_{n \in \mathcal{N}_\tau}$ from its neighborhood (e.g., $\mathcal{N}_i = \{\tau_i, \tau_k, \mathcal{L}\}$ for τ_i), which serves as input to a pre-trained policy π that determines the routing decisions.

independent routing and storage decisions under intermittent connectivity. This task is especially challenging in an unknown and complex environment like the lunar surface, further complicating the problem of reliable transmission of data packets and effective network management. As such, there is a pressing need to develop new routing algorithms for the next generation of autonomous networks and distributed robotic explorers. In this paper, we address these challenges by proposing a decentralized, learning-based communication policy where each rover makes local routing decisions based on limited neighborhood observations (Fig. 1), enabling robust multi-agent collaboration under DTN conditions.

The problem of routing in time-varying networks has seen significant interest from the community:

Delay Tolerant Networks: DTNs are communication networks designed for environments with long propagation delays and intermittent or disrupted connectivity. Their architectures introduce store-and-forward mechanisms, enabling data packets to be buffered at the source or at intermediate nodes until a suitable communication opportunity arises [2]. This paradigm is particularly relevant for the networks found in interplanetary exploration [3], where continuous End-to-End (E2E) paths rarely exist and link availability is highly dynamic. The extensive literature on the topic of routing in DTNs can be classified according to the available *information oracles* [4]. The first category comprises policies

*Federico Lozano-Cuadra and Beatriz Soret are with the Telecommunications Research Institute, University of Málaga, Spain. flozano@ic.uma.es

†Marc Sanchez Net and Federico Rossi are with the Jet Propulsion Laboratory, California Institute of Technology, Pasadena, CA USA.

‡Abhishek Cauligi is with the Department of Mechanical Engineering, Johns Hopkins University, Baltimore, MD USA.

The work of F. Lozano-Cuadra and B. Soret is partially supported by the Spanish Ministerio de Ciencia e Innovación under grant PID2022-136269OB-I00 funded by MCIN/AEI/10.13039/501100011033 and “ERDF A way of making Europe”. Part of this research was carried out at the Jet Propulsion Laboratory, California Institute of Technology, under a contract with the National Aeronautics and Space Administration (80NM0018D0004).

that rely solely on local knowledge of 1-hop neighbors. Here, random algorithms such as *Hot Potato* [5], controlled flooding algorithms like *Spray and Wait* [6], and opportunistic routing [7] are applicable. A second category includes algorithms that require knowledge of the network topology and link availability. Classical shortest path algorithms like *Dijkstra* [8] belong to this category, potentially including queueing information if available. Another family of policies depends on knowledge of node mobility. For example, *Contact Graph Routing (CGR)* predicts E2E paths for packets using pre-computed contact opportunities between all nodes in the network [9]. Finally, genie-aided oracles have full knowledge of the system, including current and future traffic demands in addition to future contact opportunities. In such cases, linear programming provides the optimal solution [4]. However, in autonomous robotic exploration scenarios, access to such information oracles is typically infeasible due to intermittent connectivity, unknown mobility patterns, and the need for decentralized decision-making, which arises naturally from these properties of the communication network. While traditional DTN routing methods perform well under specific assumptions, they face limitations in scenarios with partial observability, decentralized operation, or highly dynamic topologies. Data-driven methods can provide additional performance by learning patterns in traffic demand and contact availability, improving performance even when explicit models are unavailable or inaccurate.

Machine Learning for distributed space systems: Machine Learning (ML) techniques are increasingly being explored for autonomous decision-making in space communication systems. For planetary exploration scenarios, [10] studies the use of Federated Learning (FL) to merge the maps generated by exploring rovers in a mission concept inspired by CADRE's concept of operations. In [11], a Reinforcement Learning (RL) algorithm is proposed to autonomously manage the buffer of one node in a DTN. In [12], [13] multi-agent RL is proposed to solve the routing problem in satellite constellations, where each node of the network is an independent learning agent that makes its own autonomous routing decisions. However, the works in [12], [13] assume continuous E2E connectivity and do not incorporate store-and-forward mechanisms, rendering them unsuitable for DTNs. Additionally, their models do not support variable-sized input graphs, limiting their adaptability in dynamic multi-robot settings in which rovers may split and regroup as they explore. As a result, direct comparison with existing ML-based routing methods is not straightforward, since most rely on continuous connectivity or centralized knowledge. In contrast, Graph Attention Networks (GATs) [14] naturally accommodate changing neighborhood sizes, making them well suited for decentralized cooperation in evolving topologies. Building on graph-based methods, [15] proposes a multi-agent RL approach that processes graph-structured state information to enable decentralized satellite coordination under limited communication.

Statement of Contributions: The main contributions of this paper are: (1) we propose a rigorous decision-theoretic

model of routing over a Lunar Delay-Tolerant Network (LDTN) in the context of planetary exploration missions, applicable to any beyond-line-of-sight robotic networks; (2) we propose a novel Graph Attention-based Multi-Agent Reinforcement Learning (GAT-MARL) policy that performs decentralized routing under intermittent connectivity and partial observability; (3) we demonstrate through extensive simulations in a custom Python-based packet-level simulator that GAT-MARL outperforms classical DTN strategies, including *Spray and Wait* and *Greedy Forwarding*, while demonstrating scalability and relying only on locally observed information. *Organization:* The rest of this paper is organized as follows. In Section II, we present a rigorous model of the proposed LDTN and of its concept of operations. Section III formalizes the packet routing problem. Section IV introduces the proposed GAT-MARL framework and Section V explores its performance through extensive simulations. Finally, we conclude in Section VI.

II. SYSTEM MODEL

Figure 1 shows the considered LDTN with three primary components: (1) A team of \mathfrak{R} exploring lunar rovers; (2) a lander \mathcal{L} , serving as a base station; and (3) the map region of the lunar surface to be explored \mathcal{M} , characterized by obstacles such as craters and rocks that hinder rover mobility and communications. This system model is analogous to CADRE's [1], a planned mission which involves the deployment of three cooperative robotic explorers to the lunar surface. Although the rovers are moving and the related communication parameters change with time, we omit the time index for notation simplicity.

Each rover $\tau \in \mathfrak{R}$ is a wheeled vehicle that explores \mathcal{M} according to specific exploration objectives. During this exercise, each τ gathers information and encapsulates it in data packets $p_\tau \in \mathcal{P}_\tau$, with the global set of packets defined as $\mathcal{P} = \bigcup_{\tau \in \mathfrak{R}} \mathcal{P}_\tau$. Each rover τ is able to temporarily store packets in its local buffer \mathcal{B}_τ of capacity B , thereby forming a LDTN (Fig. 1). The joint objective of the rover team \mathfrak{R} is to maximize the number of packets $p \in \mathcal{P}$ that are transmitted to lander \mathcal{L} through the LDTN without being dropped or lost. \mathcal{L} is modeled as an infinite-capacity sink node for two main reasons: (1) it is equipped with a significantly larger buffer, $\mathcal{B}_\mathcal{L}$, and (2) it serves as a gateway to Earth, maintaining a direct, high-bandwidth (albeit intermittent) communication link that allows it to offload data as needed.

Each τ is equipped with a mesh radio module (e.g., the Microhard pMDDL used in CADRE) which supports Multiple-Input Multiple-Output (MIMO) operation and enables the establishment of direct communication links with the lander \mathcal{L} , referred to as Rover-to-Lander (r2L) links, as well as with other rovers, forming Rover-to-Rover (r2r) links. Moreover, rovers can also do store-and-forward (where τ temporarily keeps the packets in its \mathcal{B}_τ until a link to the intended destination node is available). Mathematically, the network is modeled as a time-varying graph $\mathcal{G} = (\mathcal{N}, \mathcal{E})$, where $\mathcal{N} = \{\mathfrak{R} \cup \mathcal{L}\}$ is the set of nodes, and $\mathcal{E} = \bigcup_{\tau \in \mathfrak{R}} \mathcal{E}_\tau$ is the union of all dynamically established communication links/edges. \mathcal{E}_τ is

the set of potential edges for each τ , with $|\mathcal{E}_\tau| \leq |\mathfrak{R}|+1$, as it can connect with any other $\tau \in \mathfrak{R}$ (including themselves) and with \mathcal{L} , and the local neighborhood \mathcal{N}_τ is the set containing τ and all nodes it shares a communication edge with. Together, these edges enable the formation of a dynamic wireless mesh network [16] over the lunar surface.

Exploration area: \mathcal{M} denotes the region of the lunar surface surrounding the lander that is assigned for rover exploration. This area consists of traversable terrain interspersed with obstacles such as craters and rocks that hinder rover mobility and communications. The spatial distribution and sizing of obstacles within \mathcal{M} are representative and determined using a probabilistic model calibrated with empirical lunar surface data provided by the CADRE mission.

Rover exploration: The rovers explore according to the multi-agent exploration algorithm developed for the CADRE mission. The algorithm is briefly described here for convenience and we refer the interested reader to [17] for a detailed description. An exploration episode τ starts with every $\tau \in \mathfrak{R}$ at \mathcal{L} 's position (Fig. 2). At the beginning of τ , the boundary of the region to be explored \mathcal{M} is defined (in CADRE, this is specified by ground operators [1]). \mathcal{M} is first partitioned into $|\mathfrak{R}|$ sub-regions using *K-Means* clustering (Fig. 2), and each sub-region $\mathcal{M}_\tau \subseteq \mathcal{M}$ is then assigned to a rover $\tau \in \mathfrak{R}$ using the *Hungarian algorithm* [17] to minimize the total expected travel cost. \mathcal{M} is discretized into m square cells of resolution ρ . A discrete time step t corresponds to the time it takes a rover to move from one cell to an adjacent cell. The content of \mathcal{M} is initially unknown to the rovers, and their collective exploration objective is to observe and classify every reachable portion of \mathcal{M} as “traversable” or “obstacle” using on-board stereo cameras. Each τ autonomously explores its assigned \mathcal{M}_τ using frontier-based exploration [18], [17], incrementally mapping and labeling the terrain. Every τ selects its next navigation objective among a set of frontier points independently based on a local observation, enabling decentralized and adaptive exploration throughout the region. All frontier points f are evaluated using a weighted score:

$$\text{score}(f) = w_1 \cdot d(f) - w_2 \cdot n(f),$$

where $d(f)$ is the Manhattan distance from τ to f , $n(f)$ is the information gain, i.e., the number of cells from \mathcal{M}_τ that would potentially be explored by τ along its path to f , and w_1, w_2 are tunable weights. To prevent rover collisions, obstacles are inflated using a circular footprint (Fig. 2). The chosen f becomes the next objective \mathbf{o} for τ , which computes the path towards it in advance. Frontier points are classified as unreachable if no collision-free path exists to reach them due to surrounding obstacles. The exploration episode τ ends when all the reachable points of \mathcal{M} have been classified.

Packet generation: During exploration, rovers collect imagery required for photogrammetric 3D reconstruction of the surface without human intervention and subsequently perform distributed sensing. While navigating between objectives, each rover τ collects the information and incrementally builds local maps of the surface. These maps classify regions

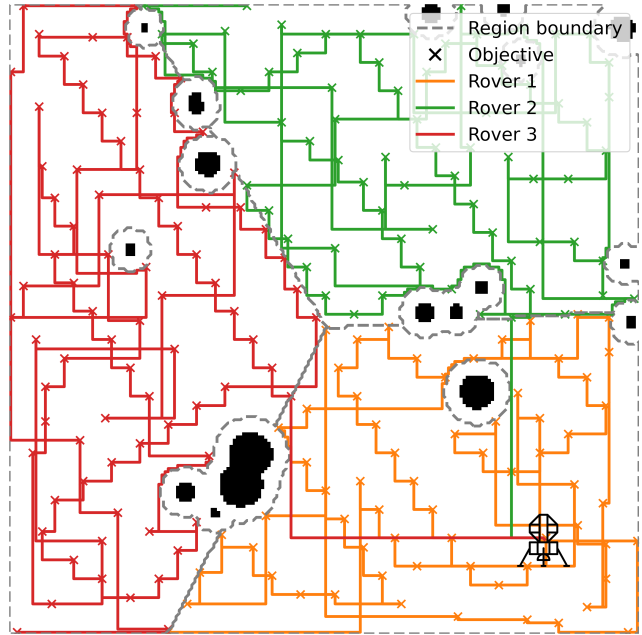


Fig. 2: The exploration region \mathcal{M} is partitioned into sub-regions, each assigned to a different rover. Rovers depart from the lander and autonomously explore their assigned areas, selecting frontier points as navigation objectives while avoiding obstacles.

as “traversable” or “obstacle” and support autonomous navigation and decision-making. Each τ periodically encapsulates this information in one packet $p_\tau(t)$ every F time steps t and stores it in its local buffer \mathcal{B}_τ . Each packet corresponds to a 1456-byte compressed traversability map, matching the telemetry format used by CADRE’s mapping component. It includes timestamps, sequence identifiers, reference vectors, orientation data, and four resolution levels of compressed binary maps, and is generated at 1Hz.

Link establishment: As the rovers move during exploration, the network topology evolves dynamically; with communication links forming or breaking over time. A communication link e_{ij} between nodes i and j is established at time t if two conditions are met: (1) The distance between nodes satisfies $d(i, j) < d^{\max}$, where d^{\max} is the maximum communication distance—a fixed parameter calibrated during pre-flight testing on Earth. This value is set depending on whether e_{ij} is $\tau_2\tau$ or $\tau_2\mathcal{L}$. (2) The path between i and j must be clear of obstructions, captured by $\text{clear}(i, j)$. Therefore:

$$e_{ij} \in \mathcal{E} \iff d(i, j) < d^{\max} \wedge \text{clear}(i, j).$$

If these conditions are satisfied with multiple nodes, a rover can maintain simultaneous active links to all such neighbors, each with its own data rate, thereby forming a dynamic mesh network. Fig. 1 illustrates the resulting topology, highlighting both available links and those that are unavailable due to either obstacles or distance limitations.

Data rate: The achievable data rate for each established link e_{ij} is denoted by $R(i, j)$ and is defined as:

$$R(i, j) = \begin{cases} R_{\tau}^{\max}, & \text{if } i, j \in \mathfrak{R} \text{ (r2r link)} \\ R_{\mathcal{L}}^{\max}, & \text{if } \{i, j\} \ni \{\mathcal{L}\} \text{ (r2L link)} \\ 0, & \text{if } e_{ij} \notin \mathcal{E} \end{cases}, \quad (1)$$

where R_{τ}^{\max} and $R_{\mathcal{L}}^{\max}$ represent the maximum achievable data rates for r2r and r2L links, respectively. As \mathcal{L} 's antenna has a higher elevation, we note that $R_{\mathcal{L}}^{\max} > R_{\tau}^{\max}$. These values are inspired by Microhard pMDL modules. Although the modules support adaptive rates, we assume constant rate links for simplicity and to focus on routing; the data rate does not vary with distance in our model.

Routing: For managing locally stored packets, each rover autonomously decides among the following actions for each packet: (1) hold packets in its buffer in order to perform store-and-forward, delaying transmission until connectivity conditions improve; (2) forward packets towards another node; or (3) generate and forward duplicate copies of packets through multiple links.

Queue Management: Each τ stores every generated packet p_{τ} in its local buffer \mathcal{B}_{τ} , which operates as a First-In, First-Out (FIFO) queue. When a new p_{τ} is created, it is appended to the end of \mathcal{B}_{τ} . If $|\mathcal{B}_{\tau}| = B$ (full), the oldest packet is dropped to make room for a new one. At each t , τ_i may transmit up to $\min(R(i, j) \cdot t, |\mathcal{B}_{\tau}|)$ packets to a selected neighbor τ_j . Packets are forwarded in FIFO order, ensuring that the oldest packets are prioritized for transmission.

III. PROBLEM FORMULATION

The routing problem involves delivering as many data packets p as possible from any rover τ to the lander \mathcal{L} through the LDTN with the limited available information on board each τ while satisfying all network constraints. Moreover, we wish to optimize energy resources while minimizing the communication overhead. We formulate the problem as:

$$\mathbf{P} : \max_{\mathbf{R}_{\tau, \mathcal{L}}^{\tau}} \sum_{p=1}^{|\mathcal{P}_{\tau}|} \mathbf{D}^p(\tau_p, \mathcal{L}), \quad \forall \tau \in \mathfrak{R}, \quad (2a)$$

$$s.t. \quad f_{ij} \leq R(i, j), \quad \forall i, j \in \mathcal{N}, \quad (2b)$$

$$|\mathcal{B}_{\tau}| \leq B, \quad \forall \tau \in \mathfrak{R}, \quad (2c)$$

where $\mathbf{D}^p(\tau_p, \mathcal{L})$ is an indicator function that equals 1 if a unique copy of packet p_{τ} generated by rover τ is delivered to the lander \mathcal{L} , and 0 otherwise. \mathbf{R}^{τ} is the set of all possible routes or paths for routing data packets during an exploration episode τ , $\mathbf{R}_{\tau, \mathcal{L}}^{\tau} \subseteq \mathbf{R}^{\tau}$ is the subset of routes that start at τ and end at \mathcal{L} to be optimized, and f_{ij} is the total flow of packets that go from node i to node j at each time step t . In the constraints, Eq. (2b) states that f_{ij} cannot exceed the capacity between the nodes, given by the achievable data rate $R(i, j)$ (Eq. (1)), limiting the usage of any given route. Eq. (2c) imposes that the number of packets stored in the buffer of rover τ , $|\mathcal{B}_{\tau}|$, does not exceed its capacity B . We note that no flow conservation constraints are imposed, since packets may be duplicated or dropped due to buffer overflows; similarly, no self-loop constraints are enforced, since rovers may perform store-and-forward.

Discussion: Solving Problem (2) requires full knowledge of present and future link availability and packet flow—information that is not accessible in decentralized exploration missions. Furthermore, agents operate autonomously with only partial observations and no access to the states observed by others, making the problem a Partially Observable Markov Decision Problem (POMDP) from each agent's perspective. We therefore address this decentralized, partially observable routing task using a RL approach under the Centralized Training, Decentralized Execution (CTDE) paradigm.

IV. LEARNING FRAMEWORK

Each rover $\tau \in \mathfrak{R}$ operates as an independent agent, making routing decisions based solely on local observations in a partially observable, dynamic environment. The proposed GAT-MARL framework follows a CTDE paradigm structured into two phases: (1) a centralized server aggregates the experiences from all rovers in a global buffer D_g to train a shared policy model π and (2) once trained, π is deployed onboard each rover, enabling decentralized execution of routing decisions without further training. This design ensures that all rovers act in coordination under the same globally optimized policy. In flight operations, no further training is expected—only the trained policy π is uploaded, and all routing decisions are made onboard fully decentralized.

We formulate the routing problem as a POMDP, defined by the tuple $(\mathcal{S}, \mathcal{A}, P(s, a), \mathcal{R}(s, a))$, with discrete time step t . At each t , a rover τ_i observes a local state $S_t^i \in \mathcal{S}$, selects an action $a_t \in \mathcal{A}$, receives a reward r_t , and transitions to a new state $S_{t+1}^j \in \mathcal{S}$ observed at the receiving node \mathbf{n}_j according to the transition probability $P(S_{t+1}^j | S_t^i, a_t)$.

The interaction model follows the innovative *packet-centric* multi-agent routing approach described in [12], [13], where the state transition from τ_i to \mathbf{n}_j after forwarding packet p is captured by the tuple: $(S_t^i, a_t^i, r_t^i, S_{t+1}^j)$, where S_t^i is observed at τ_i , and S_{t+1}^j is observed at τ_j . Unlike [12], [13], self-loops are allowed, i.e., τ_i may forward a packet to itself ($\tau_j = \tau_i$). This tuple representation is particularly well suited for decentralized routing, as learning occurs from the perspective of the packet while the model remains fully local to each rover, resulting in an efficient and communication-light implementation.

State space: At each decision step, a rover τ_i observes a local subgraph composed of itself and its 1-hop neighbor nodes $\mathbf{n} \in \mathcal{N}_{\tau}$. For each \mathbf{n} in this subgraph, a feature vector $\mathbf{x}_{\mathbf{n}} \in \mathbb{R}^7$ is constructed:

$$\mathbf{x}_{\mathbf{n}} = [\mathbb{1}_{\{\mathbf{n}=\tau\}}, \mathbb{1}_{\mathbf{n}=\mathcal{L}}, \mathbb{1}_{e_{\mathbf{n}, \mathcal{L}} \in \mathcal{E}}, \text{TTL}_{\mathbf{n}}, |\mathcal{B}_{\mathbf{n}}|, d(\mathcal{M}_{\mathbf{n}}, \mathcal{L}), d(\mathbf{n}, \mathcal{L})],$$

where each component is scaled in the range $[0, 10]$, $d(\mathbf{n}, \mathcal{L})$ and $d(\mathcal{M}_{\mathbf{n}}, \mathcal{L})$ are the Euclidean distances from \mathbf{n} and $\mathcal{M}_{\mathbf{n}}$ to \mathcal{L} , respectively. Moreover, since rovers pre-compute their path towards their next \mathbf{o} , each \mathbf{n} can predict their Time-To-Lander (TTL) value, $\text{TTL}_{\mathbf{n}}$: the number of t in which \mathbf{n} will establish a link $e_{\mathbf{n}, \mathcal{L}}$. These values form the node feature matrix $\mathbf{X}_{\tau} = [\mathbf{x}_{\mathbf{n}}]_{\mathbf{n} \in \mathcal{N}_{\tau}}$. Additionally, an adjacency matrix \mathbf{A}_{τ} encodes the bidirectional edges between the current node

and each neighbor. A TTL-masking mechanism creates an updated adjacency matrix \mathbf{A}'_t that filters neighbors with $TTL \neq 0$ whenever they are available, i.e., nodes whose path will bring them to have a communication link with \mathcal{L} . Therefore, the observed state S_t^i for agent \mathbf{r}_i is defined as the pair $(\mathbf{X}_\mathbf{r}, \mathbf{A}'_\mathbf{r})$, comprising the feature matrix of its local subgraph $\mathcal{N}_\mathbf{r}$ and the corresponding masked adjacency matrix, respectively. Overall, this design ensures that the state space \mathcal{S} remains fully local—no global topology or centralized knowledge is assumed.

Action space: At each step, every rover \mathbf{r} selects an available edge $e_{ij} \in \mathcal{E}_\mathbf{r}$ —including self-loops—to transmit packets at rate $\min(R(i, j) \cdot t, |\mathcal{B}_i|)$. This captures both forwarding and storing actions.

Rewards: The reward function is a composition of different terms that incentivize packet delivery while discouraging buffer congestion and inefficient forwarding from a rover \mathbf{r}_i to its neighbor \mathbf{r}_j . First, $r_{\text{TTL}}(\mathbf{r}_j)$ is defined as follows:

$$r_{\text{TTL}}(\mathbf{r}_j) = \begin{cases} r_{\text{noTTL}}, & \text{if } TTL_{\mathbf{r}_j} = 0 \\ r_{\text{TTL}} \cdot \frac{10^{\alpha_{\text{TTL}} \cdot TTL_{\mathbf{r}_j}} - 1}{10^{\alpha_{\text{TTL}}} - 1} & \text{otherwise} \end{cases}. \quad (3)$$

Then, the buffer usage penalty $r_B(\mathbf{r}_j)$ is defined as:

$$r_B(\mathbf{r}_j) = r_{\text{usage}} \cdot \frac{10^{\alpha_B \cdot u_{\mathbf{r}_j}} - 1}{10^{\alpha_B} - 1}, \quad (4)$$

where $u_{\mathbf{r}_j} = |\mathcal{B}_{\mathbf{r}_j}|/B$ is the normalized buffer usage at node \mathbf{r}_j . In both Eqs. (3) and (4), the reward functions follow a positive and negative exponential curve where α_{TTL} and α_B determine the steepness of each one, respectively. Therefore, the overall reward can be defined as:

$$\begin{aligned} r = & r_B(\mathbf{r}_j) + r_{\text{TTL}}(\mathbf{r}_j) \\ & + \mathbb{1}_{\{\mathbf{r}_j = R_i\}} \cdot r_{\text{hold}} + \mathbb{1}_{\{\mathbf{r}_j \neq R_i \wedge \mathbf{r}_j \neq \mathcal{L}\}} \cdot r_{\text{fwd}}, \\ & + \mathbb{1}_{\{\mathbf{r}_j = \mathcal{L}\}} \cdot r_{\text{deliver}} + \mathbb{1}_{\{\text{connected}_{\mathbf{r}_j} = 1\}} \cdot r_{\text{conn}} \end{aligned} \quad (5)$$

where, $r_{\text{noTTL}}, r_B, r_{\text{hold}}, r_{\text{fwd}} \leq 0 \leq r_{\text{TTL}}, r_{\text{deliver}}, r_{\text{conn}}$. r_{hold} and r_{fwd} are penalties for holding and forwarding packets, and r_{deliver} and r_{conn} are rewards for delivering packets to lander and to nodes that are connected to the lander, respectively.

Q-learning formulation: For the proposed decentralized routing setting, the Q-value update for rover \mathbf{r}_i selecting action a_t^i at state S_t^i is given by:

$$Q(S_t^i, a_t^i) \leftarrow (1-\alpha)Q(S_t^i, a_t^i) + \alpha \left(r_t^i + \gamma \max_{a^j} Q(S_{t+1}^j, a^j) \right),$$

where α is the learning rate, γ is the discount factor, and S_{t+1}^j is the next state observed at the receiving node \mathbf{r}_j .

Training and Loss Function: To handle function approximation and improve training stability, we adopt a Double Deep Q-Learning (DDQN) approach [19]. The Temporal Difference (TD) error is minimized via the following loss:

$$L(\theta) = \mathbb{E} \left[\left(r_t^i + \gamma \overbrace{\max_{a^j} Q(S_{t+1}^j, a^j; \theta^-)}^{\text{Target Network}} - \overbrace{Q(S_t^i, a_t^i; \theta)}^{\text{Q-Network}} \right)^2 \right], \quad (6)$$

where $Q(\cdot; \theta)$ is the online Q-network, and $Q(\cdot; \theta^-)$ the target network, updated periodically to stabilize training. Parameters θ are optimized with Stochastic Gradient Descent (SGD) over batches sampled from the experience buffer D_g .

Algorithm 1 GAT-MARL: Exploration-to-Exploitation

Initialize: Import $Q(s, a; \theta)$ and target $Q(s, a; \theta^-)$

Initialize: Set exponential decay for ε_t

```

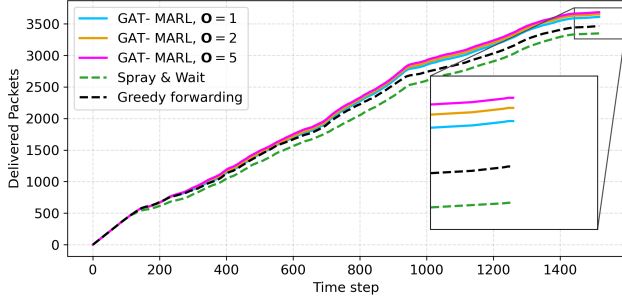
1: for episode  $t = 1, 2, \dots, \tau$  do
2:   Update network edges  $\mathcal{E}$ 
3:   for rover  $\mathbf{r}_i \in \mathcal{R}$  do
4:     Generate  $N$  information packets
5:     Observe local state  $S_t^i$ 
6:     if  $u \sim U(0, 1) < \varepsilon_t$  then
7:       Select random action  $a_t^i$ 
8:     else
9:       Select  $a_t^i = \arg \max_a Q(S_t^i, a; \theta)$ 
10:    end if
11:   Forward  $\min(R(i, j), |\mathcal{B}_i|)$  packets to  $\mathbf{r}_j$  selected by  $a_t^i$ 
12:   Compute reward  $r_t^i$  using Eq. (5)
13:   Observe next state  $S_{t+1}^j$  from  $\mathbf{r}_j$ 
14:   Store transition  $(S_t^i, a_t^i, r_t^i, S_{t+1}^j)$  in  $D_g$ 
15:   Perform SGD step using DDQN loss (Eq. (6))
16: end for
17: end for

```

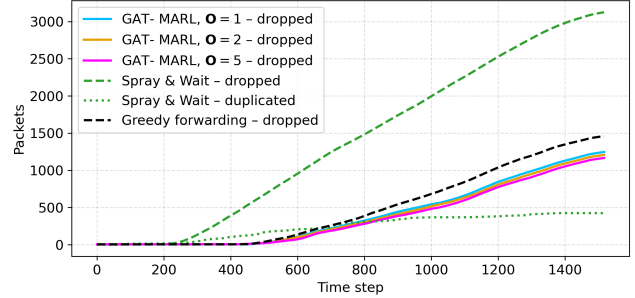
V. EXPERIMENTAL SETUP AND EVALUATION

We evaluate our approach using a custom packet-level simulator developed in Python. The simulator supports flexible modeling of lunar exploration scenarios, including obstacle-aware mobility, intermittent communication links, and data packet routing through a LDTN. Packets $p \in \mathcal{P}$ are implemented as explicit object instances, each encapsulating metadata such as the origin rover and the specific region of \mathcal{M}_p the data pertains to. We evaluated the proposed GAT-MARL policy, as well as two adapted classical non-learning strategies (*Greedy forwarding* and *Spray and Wait*). The environment setup and system components are fully aligned with the model described in Sec. II. A typical outcome of one exploration episode of duration τ is illustrated in Fig. 2.

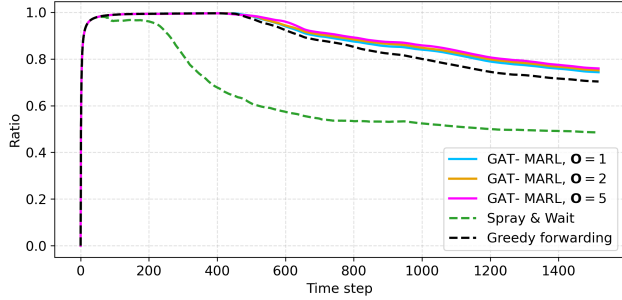
Spray and Wait [6]: This controlled flooding algorithm operates in two phases. In (1) the *Spray phase*, when a rover \mathbf{r}_i generates a new packet p_i , it initializes the packet's copy counter (which represents the maximum number of copies of the packet that will be created in the network) as $L_{p_i} = \sqrt{|\mathcal{R}|}$. When \mathbf{r}_i establishes a link e_{ij} with another rover \mathbf{r}_j , it generates and forwards a copy of the packet to \mathbf{r}_j if $L_{p_i} > 1$. The received copy p_j is assigned $L_{p_j} = \left\lfloor \frac{L_{p_i}}{2} \right\rfloor$, and the sender \mathbf{r}_i updates its packet's counter to $L_{p_i} = L_{p_i} - L_{p_j}$. Packets with $L > 1$ are considered *active* and can continue to be spread. Once $L = 1$, the packet becomes *inactive*, and (2) the *Wait phase* starts, where nodes hold the packet until they directly encounter the destination. We note that \mathbf{r}_i will not attempt to forward any packets to \mathbf{r}_j if it is



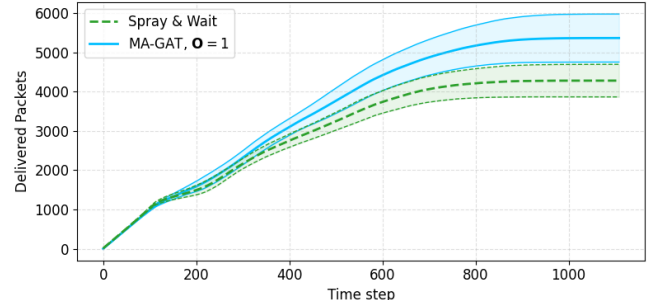
(a) Delivered unique packets.



(b) Duplicated delivered and dropped packets.



(c) Packet delivery ratio including duplicated packets.



(d) 10 rovers in 150 unseen scenarios with $\pm 1\sigma$ standard deviation.

Fig. 3: Monte Carlo comparison of *Spray and Wait*, *Greedy forwarding*, and GAT-MARL under different objective horizons \mathbf{O} . 3d shows generalization to exploration episodes τ with 10 rovers when the model was only trained on 3–5 rovers.

at capacity ($|\mathcal{B}_j| = B$). The FIFO policy is particularly valuable in this context, as it serves a dual purpose: (i) older packets are more likely to have distributed copies already, increasing delivery chances and (ii) inactive packets can only be forwarded directly to the destination, making them difficult to offload from the buffer in the absence of direct contact with the lander—a common case in LDTNs when the assigned area \mathcal{M}_{τ_i} is far from \mathcal{L} . The main advantage of this algorithm is that it operates without requiring global knowledge of the network topology or link availability—each node makes forwarding decisions based solely on its one-hop neighbors. We note that rovers avoid sending packets to neighbors that already hold a copy, assuming this knowledge is free—potentially overestimating performance.

Greedy forwarding: This method is an adaptation of the shortest path algorithm [8] for operation over a LDTN. When a rover τ_i generates a packet p_i , it attempts to compute a shortest path to the lander \mathcal{L} using the current network snapshot, i.e., the locally observed subgraph of the current connectivity state. If \mathcal{L} is reachable from τ_i in that snapshot, p_i is forwarded to the next hop τ_j along the path. Otherwise, p_i is temporarily stored in τ_i 's buffer \mathcal{B}_i . The main limitation of this approach lies in its dependence on up-to-date link state information, which requires frequent flooding of the network with control messages upon any change in topology. This overhead results in higher resource consumption and limits the scalability of the algorithm in highly dynamic networks. We note that this overhead is not modeled in our simulator: *Greedy forwarding* assumes access to up-to-date topology at no cost, which overestimates its performance.

GAT-MARL: The GAT-MARL model consists of a

lightweight 2-layer GAT followed by a fully connected prediction head. The first GAT layer uses 8 attention heads projecting input features from 32×64 to 32×512 , followed by a second GAT layer reducing it to 32×64 . A two-layer MLP head further processes the output with dimensions $64 \rightarrow 32 \rightarrow A$, where A is the number of possible actions. Dropout (20%) is applied after each layer to improve generalization. The model takes as input the feature matrix \mathbf{X}_τ and adjacency matrix \mathbf{A}'_τ (Fig. 1), and outputs one Q-value per available next-hop action. The final trained model is compact, occupying only 188KB when serialized using the PyTorch library .pt file format, requiring minimal onboard computation and energy consumption.

A Monte Carlo evaluation is performed across $\tau = 30$ exploration episodes (as shown in Fig. 2) with different maps \mathcal{M}_τ formed by randomly generated obstacle layouts and a variable number of rovers between 3 and 5 per τ . The evaluation follows a three-phase curriculum: (1) experience collection via full random actions for 10,000 steps, which are then used to train the GAT-MARL model; (2) gradual shift from exploration to exploitation at each τ , where the model is trained at every step (Alg. 1); and (3) pure exploitation under frozen policy: no training or experience collection is performed here. Each phase comprises 10 τ and each τ consists of approximately 1000–1450 time steps t , depending on the number of rovers and the obstacle distribution in \mathcal{M}_τ . Figs. 3a, 3b, 3c present the average results per τ from the final phase, where the trained model is evaluated in unseen scenarios without further learning. We compare *Spray and Wait*, *Greedy forwarding*, and GAT-MARL. For the latter, we evaluate different values of the objective horizon \mathbf{O} , defined

as the number of upcoming objectives O considered by each rover when computing its TTL. GAT-MARL achieves higher delivery rates (Fig. 3a)—with $O = 1$, it delivers 4.2% and 7.8% more packets than *Greedy* and *Spray and Wait*, respectively, and with $O = 5$, the gains increase to 6.4% and 10%, respectively. Critically, it also achieves fewer drops and no duplications (Fig. 3b), where *Spray and Wait* delivers up to 424 duplicated packets per τ on average. Finally, the proposed approach results in better delivery ratios (Fig. 3c), i.e., the number of unique packets delivered per packet created, with values of 74.35% for GAT-MARL ($O = 1$), 75.96% for GAT-MARL ($O = 5$), compared to 70.36% for *Greedy* and 48.54% for *Spray and Wait*. The performance gap widens for *Spray and Wait* due to inefficiencies from excessive packet duplication. Overall, GAT-MARL benefits from larger O values, effectively leveraging short-term mobility forecasts to improve routing.

To evaluate scalability and generalization, we test the same GAT-MARL model—trained on only 20 τ with 3–5 rovers—on 150 new τ involving 10 rovers, without any additional training. As shown in Fig. 3d, GAT-MARL clearly outperforms *Spray and Wait*, which delivers on average 4278 unique packets out of 5498, corresponding to a delivery rate of 77.8%; in contrast, GAT-MARL delivers 5362 unique packets, achieving 97.5%. This gap arises because *Spray and Wait* rapidly congests the network by creating multiple copies per packet, while GAT-MARL learns to manage congestion more effectively, keeping the network load under control, also when it is not congested. We exclude *Greedy forwarding* from the figure for two main reasons: (1) its simulated performance is similar to GAT-MARL in these scenarios; but (2) it relies on up-to-date global topology information, requiring frequent flooding of control messages—a highly unrealistic assumption in dynamic scenarios with 10 agents, where the topology changes an average of 156 times per τ . Overall, these results show that GAT-MARL holds significant promise for achieving high delivery rates without duplication or the overhead of global topology discovery, potentially enabling bolder, beyond-line-of-sight exploration for future autonomous robotic missions.

VI. CONCLUSIONS

We presented a decentralized learning-based routing framework for multi-robot exploration in LDTNs. By leveraging GATs within a multi-agent RL paradigm, our method enables each rover to make efficient, fully local routing decisions based on partial observations—without requiring global topology updates or packet duplication. The proposed GAT-MARL policy demonstrates strong performance across a wide range of simulated scenarios, consistently outperforming classical DTN baselines in terms of delivery rate, redundancy, and loss. Moreover, it generalizes effectively to larger teams without retraining, indicating its potential for scalability in future mission deployments. These results show that decentralized, attention-based policies can enable robust and scalable communication strategies in autonomous

distributed planetary networks, supporting future science-driven missions.

REFERENCES

- [1] G. Rabideau, J. Russino, A. Branch, N. Dhamani, T. . Vaquero, S. Chien, J.-P. de la Croix, and F. Rossi, “Planning, scheduling, and execution on the Moon: the CADRE technology demonstration mission,” 2025.
- [2] K. Fall, “A delay-tolerant network architecture for challenged internets,” in *Proceedings of the conference on Applications, Technologies, Architectures, and Protocols for Computer Communication*, 2003.
- [3] S. Burleigh, A. Hooke, L. Torgerson, K. Fall, V. Cerf, B. Durst, K. Scott, and H. Weiss, “Delay-tolerant networking: an approach to interplanetary internet,” *IEEE Communications Magazine*, vol. 41, no. 6, pp. 128–136, 2003.
- [4] S. Jain, K. Fall, and R. Patra, “Routing in a delay tolerant network,” in *Proceedings of the conference on Applications, Technologies, Architectures, and Protocols for Computer Communication*, 2004.
- [5] U. Feige and P. Raghavan, “Exact analysis of hot-potato routing,” in *IEEE Symp. on Foundations of Computer Science*, 1992.
- [6] T. Spyropoulos, K. Psounis, and C. S. Raghavendra, “Spray and wait: an efficient routing scheme for intermittently connected mobile networks,” in *Proceedings of the 2005 ACM SIGCOMM workshop on Delay-tolerant networking*, 2005, pp. 252–259.
- [7] M. S. Net and S. Burleigh, “Evaluation of opportunistic contact graph routing in random mobility environments,” in *Proc. IEEE Conf. on Wireless for Space and Extreme Environments*, 2018.
- [8] E. W. Dijkstra, “A note on two problems in connexion with graphs,” *Numerische mathematik*, vol. 1, no. 1, p. 269–271, 1959.
- [9] G. Araniti, N. Bezigianidis, E. Birrane, I. Bisio, S. Burleigh, C. Caini, M. Feldmann, M. Marchese, J. Segui, and K. Suzuki, “Contact graph routing in DTN space networks: overview, enhancements and performance,” *IEEE Communications Magazine*, vol. 53, no. 3, pp. 38–46, 2015.
- [10] T.-I. Szatmari and A. Cauligi, “Federated multi-agent mapping for planetary exploration,” 2025. [Online]. Available: <https://arxiv.org/abs/2404.02289>
- [11] E. Harkavy and M. S. Net, “Utilizing reinforcement learning to autonomously manage buffers in a delay tolerant network node,” in *IEEE Aerospace Conference*, 2020.
- [12] B. Soret, I. Leyva-Mayorga, F. Lozano-Cuadra, and M. D. Thorsager, “Q-learning for distributed routing in LEO satellite constellations,” in *Proc. IEEE Int. Conf. on Machine Learning for Communication and Networking*, 2024.
- [13] F. Lozano-Cuadra, B. Soret, I. Leyva-Mayorga, and P. Popovski, “Continual deep reinforcement learning for decentralized satellite routing,” *IEEE Transactions on Communications*, pp. 1–1, 2025.
- [14] P. Veličković, G. Cucurull, A. Casanova, A. Romero, P. Lio, and Y. Bengio, “Graph attention networks,” *arXiv preprint arXiv:1710.10903*, 2017.
- [15] S. Dolan, S. Nayak, and H. Balakrishnan, “Quantifying impact of information sharing on satellite navigation,” *AIAA Journal of Guidance, Control, and Dynamics*, 2025.
- [16] M. Saboia, F. Rossi, V. Nguyen, G. Lim, D. Aguilar, and J.-P. de la Croix, “CADRE MoonDB: Distributed database for multi-robot information-sharing and map-merging for lunar exploration,” in *Int. Workshop on Autonomous Agents and Multi-Agent Systems for Space Applications*, 2024.
- [17] S. Nayak, G. Lim, F. Rossi, M. Otte, and J.-P. de la Croix, “Multi-robot exploration for the CADRE mission,” *Autonomous Robots*, vol. 49, no. 2, p. 17, 2025.
- [18] B. Yamauchi, “A frontier-based approach for autonomous exploration,” in *Proc. IEEE Int. Symp. on Computational Intelligence in Robotics and Automation*, 1997.
- [19] H. Van Hasselt, A. Guez, and D. Silver, “Deep reinforcement learning with double Q-learning,” in *Proc. AAAI Conf. on Artificial Intelligence*, 2016.